



## A SECOND GENERATION NARROW BAND NEUTRINO BEAM

D. A. Edwards and F. J. Sciulli

May 1976

### INTRODUCTION

In this memorandum, we present a design for a new narrow band neutrino beam. It may be called a "second generation" design with some justification, for in experimentation throughout the past four years the virtues and limitations of the existing narrow band beam<sup>1</sup> have been thoroughly explored.

The promise of the narrow band concept has indeed been realized in a number of ways, from the ability to produce neutrino flux at a well defined mean energy to the demonstration of the neutral current signal by observation of low energy hadron showers without accompanying muons. Event rates are quite acceptable at high energy. For example, during a recent run the beam was set for positive secondaries of mean energy 250 GeV with 400 GeV protons incident on the target. The rate for a 170 ton neutrino target at the Wonder Building was about 2 events for kaon neutrinos and about 3 events for pion neutrinos for  $10^{14}$  protons striking the primary target. The neutrino spectrum for this circumstance, as calculated by the program NUADA,<sup>2</sup> is shown in Figure 1.

Fruitful as this research has been, the pursuit of many physics questions is limited by certain features of the old beam. In descending order of relative importance, these characteristics may be listed as follows:

1. Limitation in secondary energy to 250 GeV.
2. Wide band neutrino background from meson decays upstream of the decay tube.
3. Difficulties in dumping of the primary proton beam for certain secondary energies.
4. Overly broad momentum acceptance.

In the next section, we elaborate on these points and their influence on the physics program. We then describe a new beam configuration and discuss how it faces up to these problems.

## LIMITATIONS OF THE OLD BEAM

The magnet layout of the existing narrow band beam is shown in Figure 2, together with a selection of its parameters.

### 1. Limitation in Secondary Energy

The single most important factor affecting the neutrino event rate is the accelerator energy. For a secondary beam setting at a fixed fraction of the proton energy  $E_0$ , event rates for kaon neutrinos vary roughly as  $E_0^3$  to  $E_0^4$  for the conditions considered here. Rates for the less energetic pion neutrinos do not vary as steeply, thus an increase in accelerator energy accompanied by a proportionate increase in the capability of the secondary beam system not only raises the absolute rate but also improves the kaon to pion neutrino event ratio.

Adequate event rates are obtained from kaon neutrinos for kaons of energy up to about 2/3 that of the protons and from kaon anti-neutrinos for kaons up to about 1/2 of the proton energy. The maximum secondary energy of 250 GeV in the old beam was a reasonable match to the 400 GeV peak accelerator energy and to the shielding upstream of the Wonder Building. We anticipate future running at the Lab-E location at higher accelerator energies than available in the past. A proton beam energy of 500 GeV should imply a narrow band beam operable in the neighborhood of 350 GeV. The present shield forward of Lab-E should be sufficient for muon energies in excess of 400 GeV. Substitution of steel in place of some of the earth or the use of magnetic shielding could make it possible to experiment with any secondary energy from protons of up to 1000 GeV.

### 2. Wide Band Background

Meson decays upstream of the decay tube entrance lead to the so-called wide band neutrino background in what would otherwise be a dichromatic spectrum. This situation is illustrated in Figure 3, which shows the anti-neutrino flux arising from decays within the decay tube with the present beam tuned to a "worst case" condition - focusing for negatives at 200 GeV with 400 GeV protons incident. Underlying the signal (even exceeding the signal at the lowest energies) is the background, composed of

both neutrinos and anti-neutrinos, from meson decays before the decay tube. The calculations underestimate the background in the critical low energy region; however, it is found experimentally that the background is within about a factor of two of that shown, relative to the signal neutrinos.

This background is the most serious obstacle in measuring the hadron energy distribution for neutral current interactions. In order to obtain a clean unbiased sample of neutral current events, the contribution to the rate from decays upstream of the decay tube must be subtracted. This is done experimentally by closing a slit upstream of the decay region, measuring the apparent neutral current rate under these conditions, and then performing a subtraction. In principle, this is an unbiased procedure, but the subtraction is large for anti-neutrinos, amounting typically to about 30%. This means that the statistical level of the data per hour of running time is about a factor of two worse in comparison to a negligible background case. In addition the relative normalization between the raw and subtracted data sets must be monitored with extreme care.

It must be emphasized that the severity of the background is not measured by a comparison of the signal and background fluxes at the same neutrino energy. In neutral current studies, the problem is that rather inelastic interactions of low energy background neutrinos are indistinguishable from relatively elastic high energy neutrino events. Later, we will introduce a quantitative criterion for background evaluation, in order to compare beam designs.

### 3. Dumping of the Incident Proton Beam

Over a significant fraction of the secondary energy range, the primary beam would strike the last quadrupole. In order to prevent this condition, a beam dump just upstream is lowered to intercept the protons; however the dump severely restricts the solid angle acceptance. Thus, for example, with 400 GeV protons incident, the secondary energy range from 135 GeV to 180 GeV is accessible only with an unfortunate flux limitation.

### 4. Momentum Acceptance

The source of the problems grouped under this heading is

indicated in Figure 4, which shows the vertical (bend plane) and horizontal angular acceptances for a point target as a function of the momentum deviation,  $\Delta p/p_0$ , from the central momentum  $p_0$  of the secondary beam. In the vertical plane, the angle and momentum slits are set at  $\pm 1$  inch and  $\pm 2$  inches respectively; the limits in the horizontal plane are defined by magnet apertures.

The small momentum dispersion of the old beam leads to the gentle slope of the momentum slit projections in Figure 4a. A high momentum tail extends to +100% in  $\Delta p/p_0$ . This tail creates serious difficulty in hadron beam monitoring, for, with the beam set to accept positive particles, a profusion of high energy diffracted protons traverses the decay tube, enters the monitoring equipment, and swamps the meson signal. The determination of normalized cross sections is impractical in this circumstance. The procedure in the past has been to raise the lower angle slit to the position represented by the dashed line in Figure 4a. The tail is thereby shortened, at the expense of a serious reduction in angular acceptance.

The relative solid angle acceptance versus momentum is shown in Figure 5a. The full width at half maximum is 37%. A sharper energy resolution would be desirable in order to obtain a narrower peak from kaon decays, as well as to eliminate tails.

A third feature of the acceptance function which deserves improvement is the angular dispersion of off-momentum secondaries in the decay tube - primarily a consequence of chromatic aberration. Figure 5b shows the range of angles of particles upon entry to the decay tube, for slits placed as in Figure 4. For example, at  $\Delta p/p_0 = -20\%$ , a momentum deviation for which the acceptance is still relatively large, the angular range of secondaries in the horizontal plane is  $\pm 1$  mrad. At the end of the decay tube, some 1200 feet downstream, this angular range translates into a width of 2.4 feet, further complicating the process of hadron flux monitoring.

## THE NEW BEAM

### 1. Difference from Old Beam

The differences are quantitative rather than qualitative; the focusing systems are conceptually the same. The meson production target is placed at the focus (in both planes) of a quadrupole doublet. In order to achieve parallelism of outgoing rays with momenta close to the central momentum, bending magnets are placed within the doublet with compensating bends downstream of the doublet.

The major distinctions are as follows. As suggested in the preceding section, the design value of the secondary energy is taken to be 350 GeV. In order to reduce the neutrino background originating near the target, the targetting angle has been raised to approximately 12 mrad - double that of the old beam. The larger targetting angle will lead to an increase in the momentum dispersion; a further enhancement of the dispersion has been effected by placing a "dog-leg" bend downstream of the doublet. As a result of these steps, the problem in the old beam of the intrusive dump no longer exists, for the density of magnets is such that there is no place to put it. Instead, beam dumping must occur within the magnets.

The increased targetting angle implies larger lateral excursions of the beam line. In order that the system fit comfortably within the target tube, the bend plane is horizontal.

We will discuss two versions of the design. One, referred to as the "flat" beam, will have bending in only the horizontal plane. The other, referred to as the "twisted" beam, will have small excursions in the vertical plane as well in order to reduce the wide band background further. The same longitudinal distribution of magnets is used in the two versions; the vertical bends in the second are made by rotation of dipoles about the beam direction.

### 2. Layout and Description

For this study, we have assumed the use of main ring magnets. These are compact high field magnets of a familiar and highly developed design - the selection of an established design should minimize procurement time and facilitate replacement. Where

necessary, however, we have introduced half-length (ten foot) dipoles. The number and disposition of magnets have been selected so that no magnet current will exceed 5000 A with the beam line set to select mesons of 350 GeV/c momentum.

The magnet characteristics and coordinates are listed in Table 1 and the layout is sketched in Figure 6. The z-axis passes through the target and is directed parallel to the central trajectory at its exit from the system. The positive x-axis points in the direction of site west; the positive y-axis points upward. The target center is located at the origin of coordinates. Upstream of the target, dipoles deflect the incident beam so that it strikes the target at an angle of 12.2 mrad with respect to the decay tube axis. To facilitate description, we will assume that this angle is directed from east to west. The output beam from the system is directed at an angle of 0.5 mrad westerly with respect to the axis of the decay tube in order that the beam may exit the decay tube near its center. With respect to our z-axis, the targetting angle is therefore 11.7 mrad. In the case of the twisted version, an additional upward targetting angle of 1 mrad is presumed.

Space requirements of the magnets are based on data given by T. Toohig;<sup>3</sup> neighboring magnets are separated by a gap of 5.6 inches. The layout is intended to be consistent with division into the twenty foot modules of the Neutrino Department trains. The beam rests on nine bed-plates, the last of which is 10 feet from the beginning of the decay tube. The target is three to four feet within the target tube.

The first five quadrupoles form the vertically focusing lens of the doublet. They can be excited in series; at 350 GeV/c, the current requirement is 4600 A for the magnet spacings given. The center lines of these five quadrupoles are offset with respect to the central trajectory so that they act as combined function magnets, bending in the same sense as the first three dipoles. This arrangement is motivated less by the bending obtained than by the desire to increase the space within the magnets for absorber to the side of the aperture on which beam dumping will occur.

The last pair of quadrupoles represent the horizontally focusing

lens, with an excitation current of 4500 A at 350 GeV/c. Their axes coincide with the central trajectory and they are not required to play a role in beam dumping.

The first two dipoles each bend in an easterly sense by 4.4 mrad, and the five offset quadrupoles produce a total easterly bend of 5.6 mrad. This total bend angle of 14.4 mrad (and the slope to the momentum dispersion that is produced thereby) is compensated by the last 10 foot dipole which bends 2.7 mrad to the west to direct the output beam in the desired manner. The dog-leg provided by the two 20 foot dipoles - 8.8 mrad each - assists in improving momentum selection. The choice of 8.8 mrad is natural, since then four of the dipoles can be in a single series circuit (4300 A at 350 GeV/c). Horizontal steering can be performed by fine adjustment of the 2.7 mrad bend.

For the twisted beam, with its additional vertical targetting angle of 1 mrad, two of the dipoles are rotated to provide vertical bending. The second dipole is rotated through an angle of  $37^\circ$  to produce a further upward bend of 3.3 mrad. The 3.3/1 ratio between this second dipole bend and the targetting angle is determined by the focusing optics; a final 4.3 mrad bend in the downward sense effected by rotation of the third dipole will result in zero slope of the vertical momentum dispersion function and bring the beam level. To simplify the discussion in this paper, it is assumed that the excitations of these two magnets are increased to preserve the horizontal plane geometry. It is likely that, in actual construction of the twisted beam, an adjustment of the transverse geometry would be made in order to permit series powering of the four dipoles.

Beam dumping takes place in the first seven magnets. Since the horizontal aperture is limited by magnets downstream of them, absorbers may be placed in these magnets to intercept the primary proton beam after it passes through the production target. The horizontal aperture requirements listed in Table 1 are consistent at the condition that the angular acceptance in this plane be  $\pm 1$  mrad over a source 5 mm in lateral extent. The 5 mm figure is intended to include allowance for proton beam size, centering of the beam on the target, and alignment uncertainty. The center

lines of the first two quadrupoles are displaced west by 1.32 inches with respect to the beam center. Thus, in QV1 for example, there is space for about 3.4 inches of absorbing material between the west edge of the aperture and the coil.

### 3. Calculated Performance

Consider first some aspects of the secondary hadron beam. The upper portion of Figure 7 shows rays at the central momentum projected with initial angles and displacements in the two transverse planes. As would be expected, there is no significant difference between this plot and a corresponding one prepared for the old beam. However, the momentum dispersion function evaluated at the central momentum, plotted in the lower part of Figure 7, has a value at the end of the beam 2.5 times that of the old beam.

The effect of the higher momentum dispersion is indicated in Figure 8, showing angular acceptance versus momentum deviation from the central momentum. Figure 8 is to be compared with Figure 4 for the old beam; note, however, that the momentum scale has been expanded by a factor of two in Figure 8. The high momentum tail now extends less than half as far as that associated with the old beam, without sacrifice of solid angle acceptance at the central momentum.

The angular acceptances for a point target of Figure 8 project to the transverse position boundaries at the end of the decay tube shown in Figure 9a. Though the excessive displacements associated with low momentum particles produced at the larger non-bend plane angles still exist, a significant improvement has been made by the sharper low momentum cutoff. The magnifications as a function of momentum deviation are plotted in Figure 9b. While a modest reduction of the large non-bend plane magnification as compared to the old beam results from spreading out the first thick lens of the doublet, the sensitivity to non-bend plane proton beam position will be much the same as the existing beam.

Strictly speaking, Figures 8 and 9 pertain only to the flat beam; the second rotated magnet, D3, of the twisted beam presents a sloped aperture limit. Its effect is indicated in Figure 10. Figure 10a shows the relative solid angle acceptance of the two versions, normalized to unity at  $(\Delta p/p_0) = 0$  for the flat beam. In Figure 10b

we plot the relative acceptance of 350 GeV/c pion secondaries,<sup>4</sup> again normalizing to unity at the central momentum for the flat beam. The integrals under the twisted beam curves in Figures 10a and 10b are 73% and 90% respectively of the corresponding integrals under the flat beam curves. The fraction accepted of pions produced at the central momentum versus the energy setting of the beam is shown in Figure 11a. As part of the final adjustment of the transverse geometry of the beam, it may be appropriate to reduce the vertical targetting angle somewhat to improve the acceptance of the twisted beam. With a vertical targetting angle of 1 mrad, the 4.3 mrad vertical bend required of dipole D3 implies a rotation of  $26^\circ$  about its axis. The restriction imposed by the slanted aperture decreases rapidly with angle, as sketched in Figure 11b. With the same longitudinal distribution of magnets, other combinations of vertical bends are possible and merit study.<sup>5</sup>

To compare neutrino fluxes, let us again consider the difficult situation of negative secondaries at 200 GeV with 400 GeV protons on the target. At the Lab-E location, the anti-neutrino signal and neutrino + anti-neutrino background that would be produced by the old beam appear in Figure 12. In order to maximize the signal to background ratio, the slits of the old beam are wide open. The corresponding results for the flat and twisted versions of the proposed beam are presented in Figures 13 and 14.

The improved momentum selection of the proposed beam leads to a marked sharpening of the peaks, as desired. The smaller momentum acceptance also reduces the signal fluxes; however, the increased target mass in Lab-E and access to higher energies will roughly compensate for the lower flux insofar as absolute rate is concerned.

Of greater significance is the progressive lessening of the wideband background through this set of figures. The increased targetting angle leads to most of the difference between the backgrounds of the old and flat beams; mesons produced near the target are less likely to direct neutrinos toward the experimental equipment. The "wrong sign" background - neutrinos, in this case - is suppressed particularly effectively. Though the right sign (anti-neutrino) background is also substantially reduced below

50 GeV, the flat beam yields little or no improvement above 50 GeV.

This latter circumstance is not surprising, for the background above 50 GeV or so arises from mesons that enter the beam transport and which have much lower energies than the energy for which the beam is set. These mesons are bent by the magnets through angles larger in inverse proportion to their momentum, so that even though the higher momentum central trajectory may be directed at a substantial angle with respect to the detector system, low energy particles at the same longitudinal position can be pointed directly at the detector. Since the low energy component is produced in greater abundance and has a shorter lifetime, their decays produce a significant background before the mesons strikes the walls of the aperture. The vertical excursions of the twisted beam were introduced in order to prevent these mesons from "looking" at the detector; while they are being bent toward the experiment in one plane, they are deflected away in the other. The beneficial consequence may be seen by comparison of Figures 13 and 14.

The value of these background reductions can be illustrated by considering a particular experiment - the measurement of the inelasticity distribution in neutral current interactions. If the background flux at a neutrino energy  $E_\nu$  is denoted by  $B(E_\nu)$ , then the event rate varies as  $E_\nu B(E_\nu)$ . For a distribution independent of the inelasticity  $y$ , these events would yield a hadron energy distribution flat from 0 to  $E_\nu$ . The fraction above a hadron energy cutoff of, for example, 15 GeV would then be  $(E_\nu - 15)/E_\nu$ . Multiplying these factors and summing gives  $\int (E_\nu - 15) B(E_\nu) dE_\nu$  as a relative background measure. The integrals evaluated for Figures 12, 13, and 14, are in the ratios 13/2.2/1. The twisted beam, therefore, shows promise of cutting the 30% background rate mentioned in the section on the old beam to below the 5% level after taking into account the smaller signal flux.

Figure 15 shows the signal and background neutrino fluxes with the twisted version of the new beam accepting positive 250 GeV secondaries for 400 GeV protons. Note that the signal from kaon decays is essentially the same as that of Figure 1, for the old

beam was operated with reduced aperture when tuned for positives. Again, a marked reduction in wideband background has been obtained.

As a final illustration of neutrino fluxes, we show in Figure 16 the kaon neutrino signal incident on a cylindrical detector 42 cm in radius concentric with the beam axis under the same circumstances as Figure 15. In comparison with Figure 15, the peak of Figure 16 is narrower and at a higher energy. Similar plots for a series of concentric shells of the detector in effect resolve the broad distribution of Figure 15 into a set of narrow peaks the energy of which decreases with increasing radius. A knowledge of the radial position of the event vertex thus permits an improved definition of the neutrino energy.

In conclusion, the beam design outlined above makes substantial improvements in those areas of concern identified at the outset of this memorandum. It also offers the potential of still higher energy operation, beyond the level considered here, as may be appropriate if the Energy Saver/Doubler comes into operation before major modifications are made in the experimental areas. By raising the excitation of the magnets to the same current as that at which they operate in the main ring at 500 GeV, the beam could be tuned for secondaries at 430 GeV - a reasonable match to a 700-GeV Energy Saver/Doubler. Still higher energies can be contemplated by a readjustment of the transverse geometry and movement of the primary target into Neuhall. Though the latter steps imply some cost in both funds and performance, they may provide an avenue for a first look at narrow band neutrino physics with 1000 GeV protons.

#### ACKNOWLEDGEMENTS

We are grateful to R. Lundy, S. Mori, and D. Theriot of the Neutrino Department for many valuable discussions, and to Y.K. Chu for his assistance in the neutrino flux calculations.

#### REFERENCES

1. NAL Proposal E21, F. Sciulli et al, June 10, 1970, P. Limon, et al, Nuclear Instruments and Methods 116, 317 (1974)
2. The program NUADA has been developed by D. Carey. The Hagedorn-Ranft spectrum is used as input for the calculations of this paper.

3. T. Toohig, Fermilab TM-632, December 5, 1975
4. For these estimates, we employ an angular distribution for inclusive pion production of the form  $d\sigma/dp_{\perp}^2 = (A/a)e^{-ap_{\perp}^2} + (B/b)e^{-bp_{\perp}^2}$  with  $A = 0.59$ ,  $a = 15/\text{GeV}^2/c^2$ ,  $b = 2.7 \text{ GeV}^2/c^2$ ,  $B = 1-A$ .
5. S. Mori has informed us that he has obtained a further reduction in wideband background by rotating dipole D1, with a smaller rotation of the aperture limiting dipole D3 than in the case of our twisted version.

TABLE 1. Magnets and their characteristics for the proposed beam. Location of magnet centers along beam is specified by z coordinate; transverse location of central trajectory given by x and y. Vertical (y) values pertain to the twisted beam. Quadrupole power is  $B'L/B_0$ . Free aperture required in horizontal plane is shown for magnets in which beam dumping will take place.

Name	Type	z(ft)	x(in)	y(in)	Power	Aperture	Comments
D1	10' B1	5.77	0.81	0.07	4.4 mr	±0.24"	
QV1	7' Quad	15.00	1.62	0.18	-.0138/ft 1.5 mr	±0.38	Axis displaced 1.32" west
QV2	7' Quad	22.67	2.16	0.27	-.0138/ft 1.5 mr	±0.50	Axis displaced 1.32" west
D2	10' B1	31.90	2.63	0.38	4.4 mr 3.3 mr*	±0.75	*Vertical bend for twisted beam
QV3	7' Quad	41.13	2.62	0.86	-.0138/ft 1.0 mr	±0.96	Axis displaced 0.88" west
QV4	52" Quad	47.46	2.54	1.19	-.0085/ft 0.62 mr	±1.12	Axis displaced 0.88" west
QV5	7' Quad	53.79	2.41	1.51	-.0138/ft 1.0 mr	±1.56	Axis displaced 0.88" west
QH1	7' Quad	68.21	1.94	2.26	0.0135/ft		
QH2	7' Quad	75.88	1.69	2.65	0.0135/ft		
D3	20' B1	90.08	1.23	3.38	8.8 mr -4.3 mr*		*Vertical bend for twisted beam
D4	10' B1	152.73	-7.42	3.38	-2.7 mr		
D5	20' B1	168.50	-9.09	3.38	-8.8 mr		

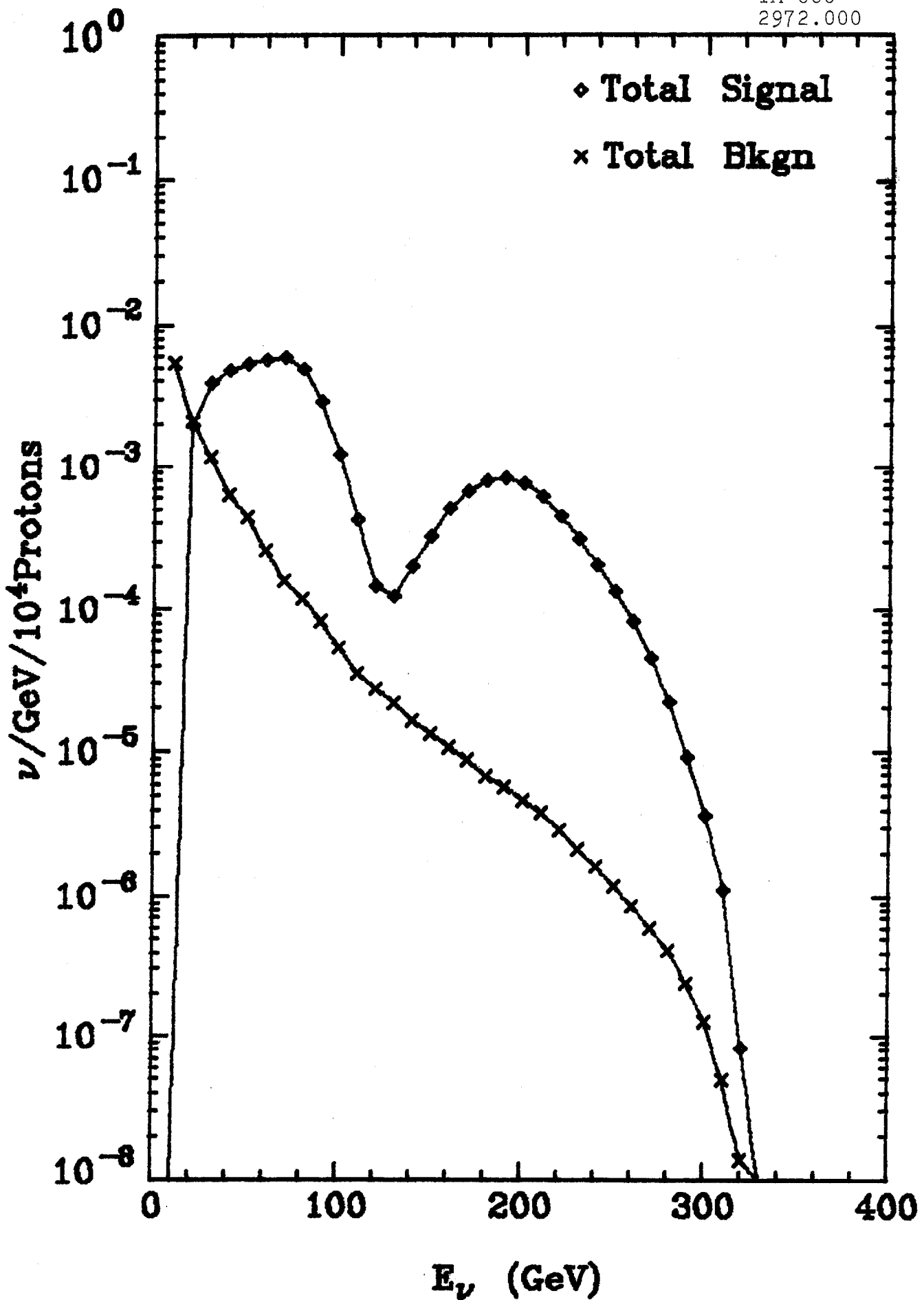
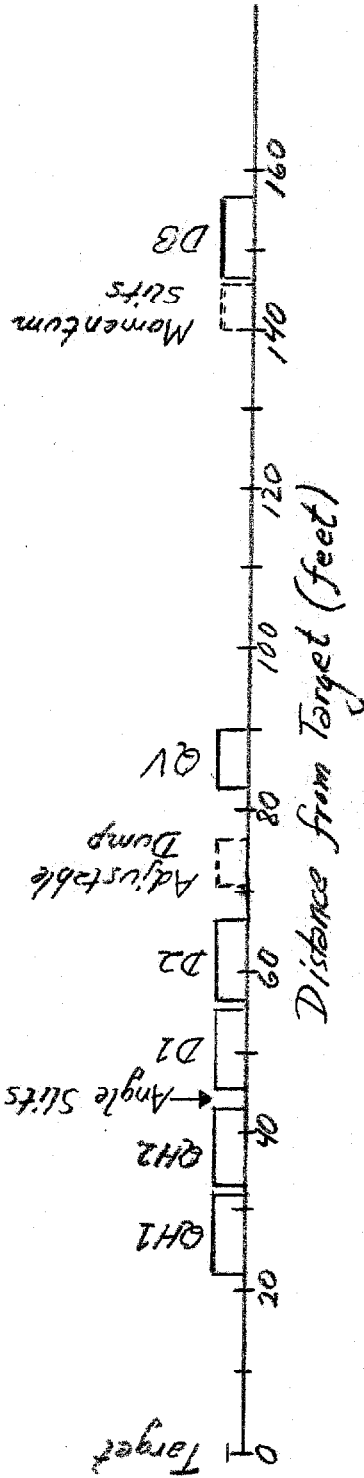


Figure 1. Signal and background neutrino fluxes at Wonder Building location with old narrow band beam set to accept positive secondaries at 250 GeV for 400 GeV incident protons.



Magnets

- QH1, 2 EPB Quads  $B'L/Rp = -0.024/\text{ft.}$
- QV MR 7' Quad  $B'L/Rp = 0.015/\text{ft.}$
- D1, 2 EPB Dipoles 6 mrad bend each
- D3 EPB Dipole - 6 mrad bend

Maximum Energy 250 GeV  
 Targetting Angle 6 mrad (vertical)

Acceptances	Angular (at $E_0$ )	$\Delta P/P_0$ (FWHM)
Angle slits $\pm 1''$	$\pm 1.0(V), \pm 2.4(H)$ mr	37%
Angle slit $+1'', -0.2''$	$+1.0, -0.3(V), \pm 2.4(H)$	24%

Figure 2. Layout of old narrow band beam and summary of characteristics.

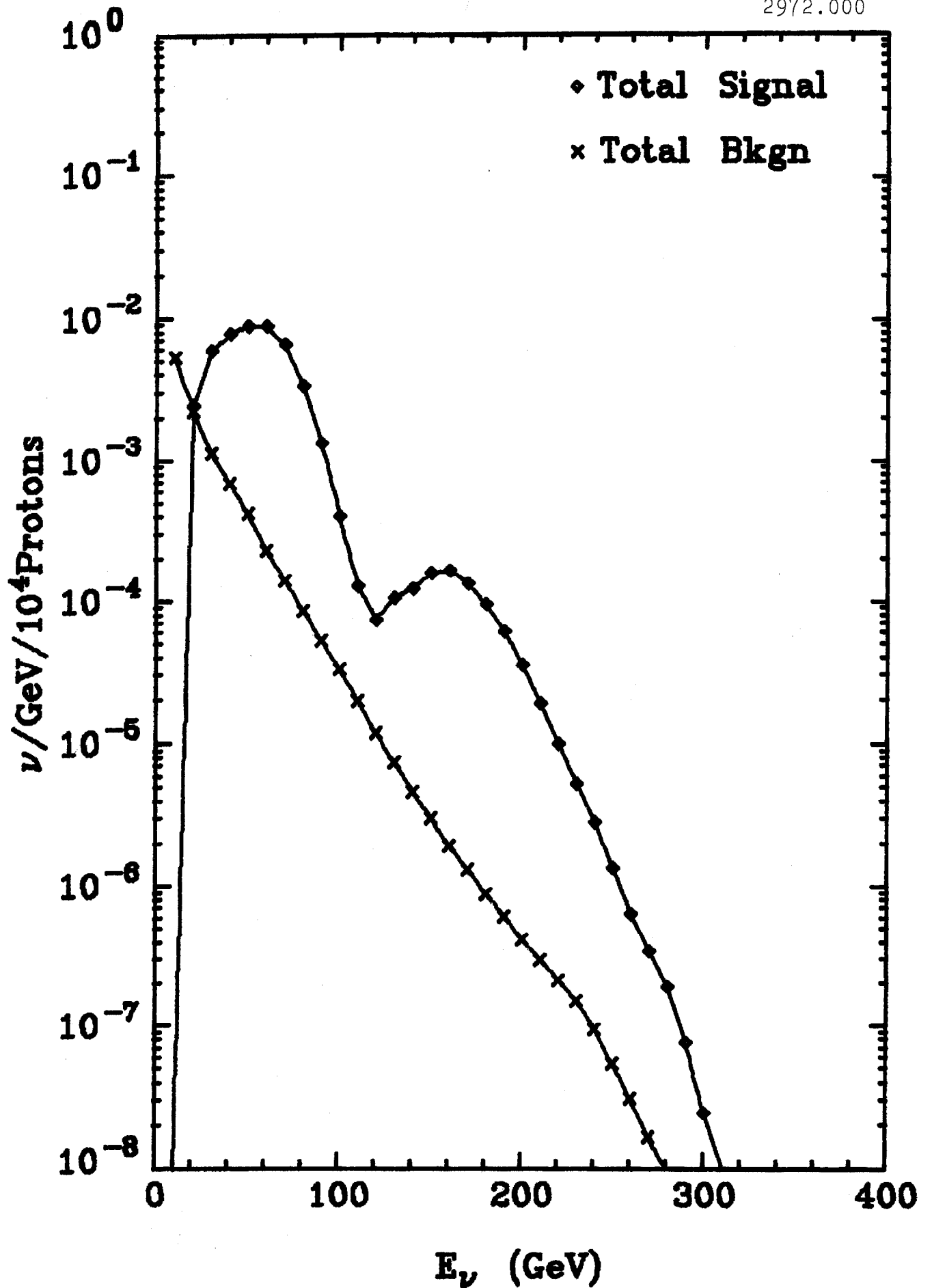
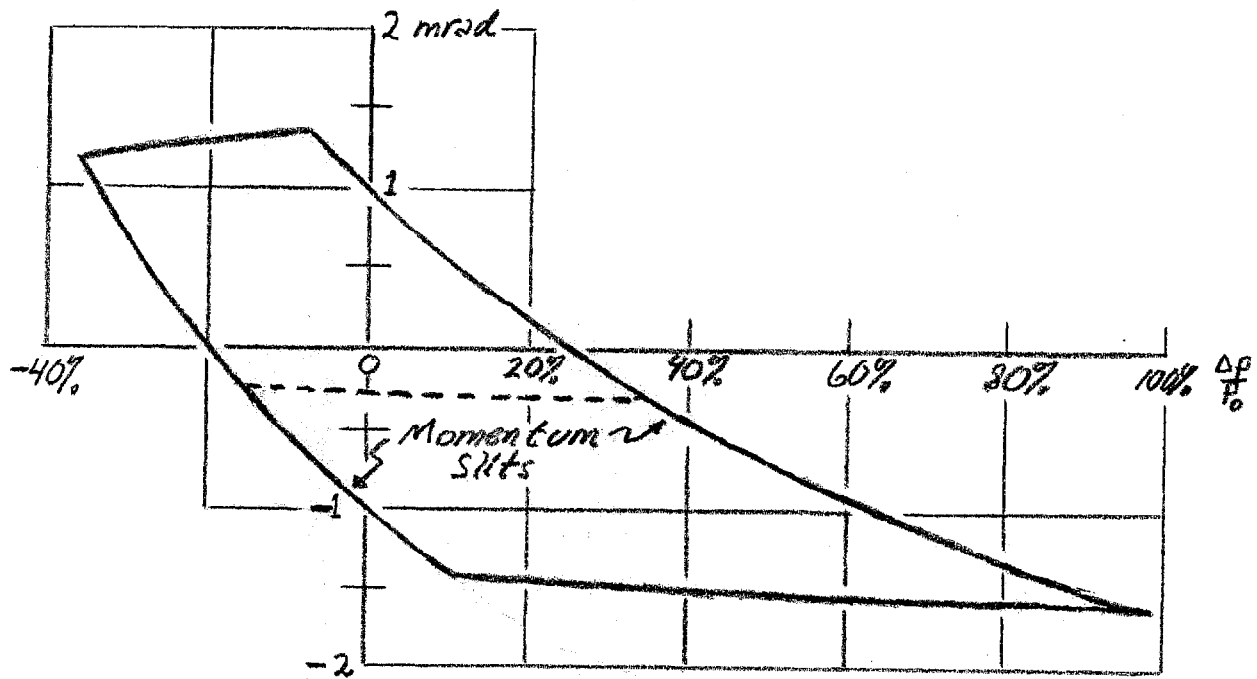
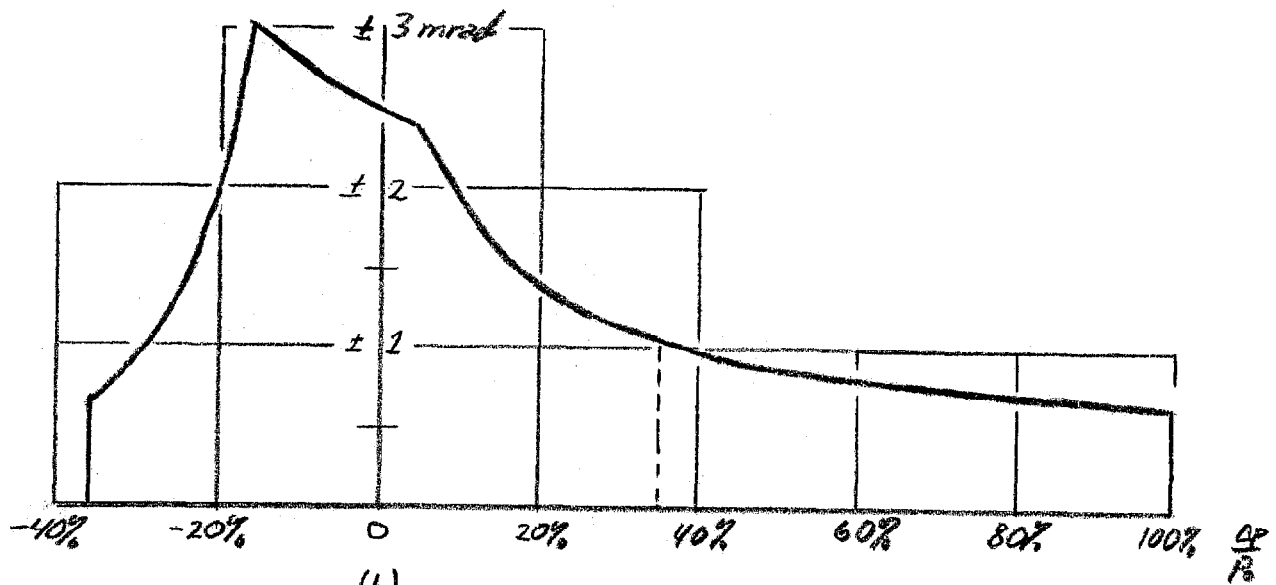


Figure 3. Signal and background neutrino fluxes at Wonder Building location with old narrow band beam set to accept negative secondaries at 200 GeV for 400 GeV incident protons.



(a)



(b)

Figure 4. Angular acceptance versus momentum for old beam in (a) vertical plane, and (b) horizontal plane.

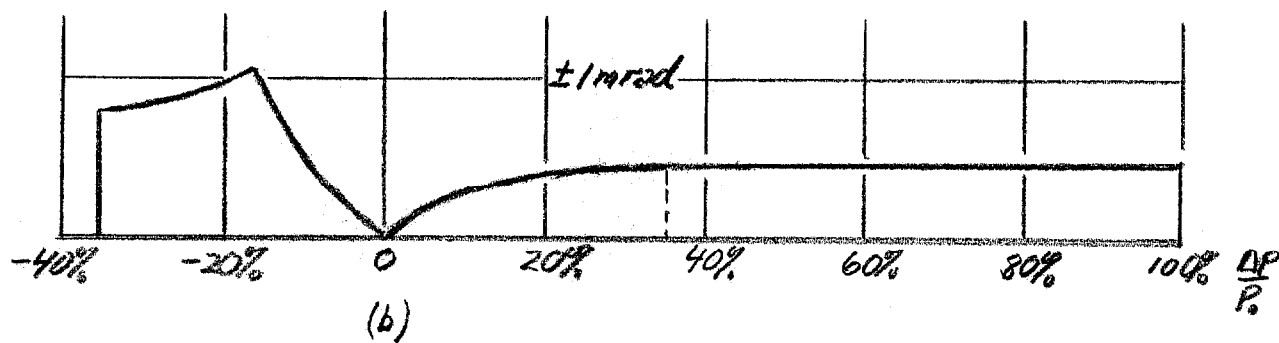
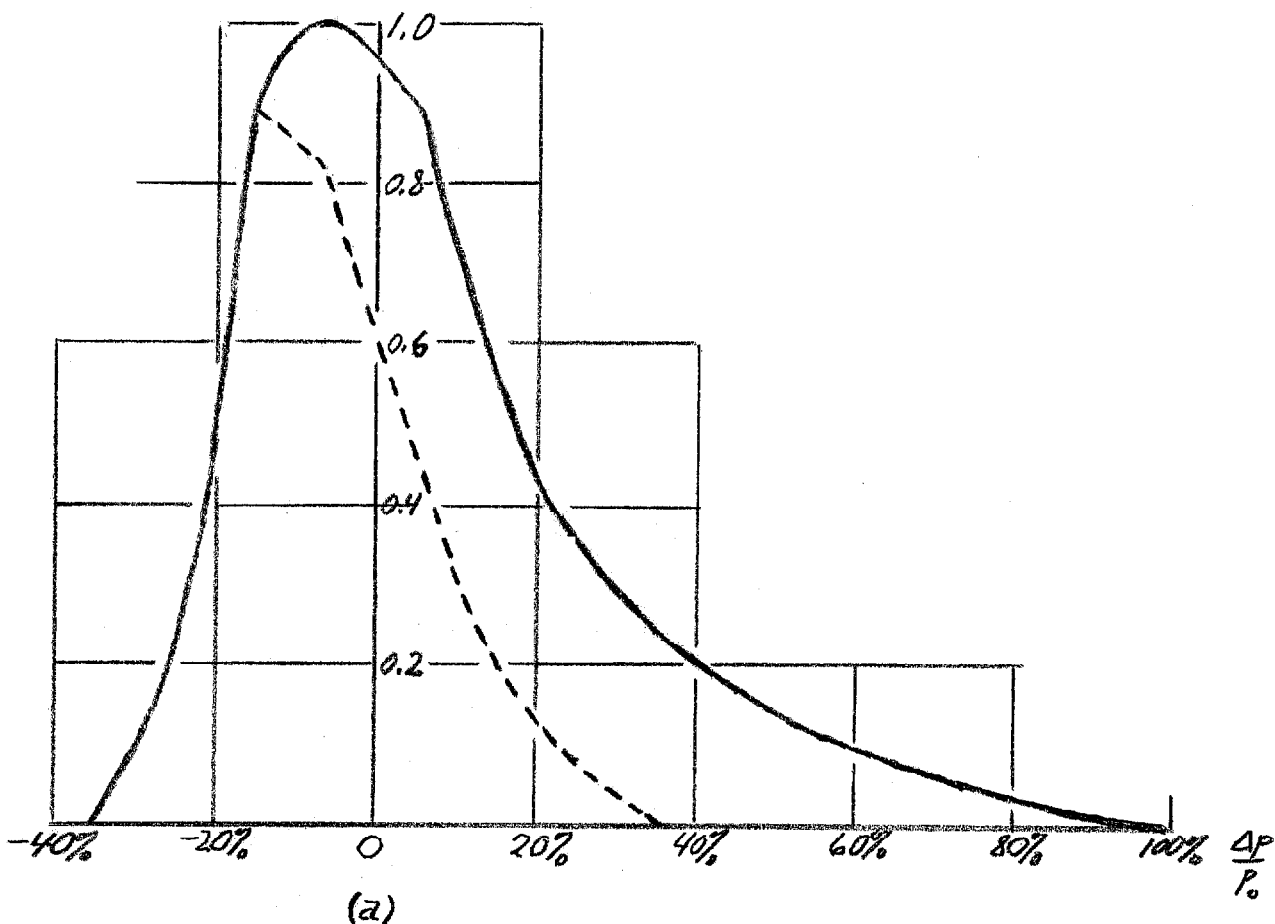


Figure 5. (a) Relative solid angle acceptance of old train versus momentum. Lower angle slit in position to cut off high momentum represented by dashed curve. (b) Boundary of exit angle distribution in horizontal plane.

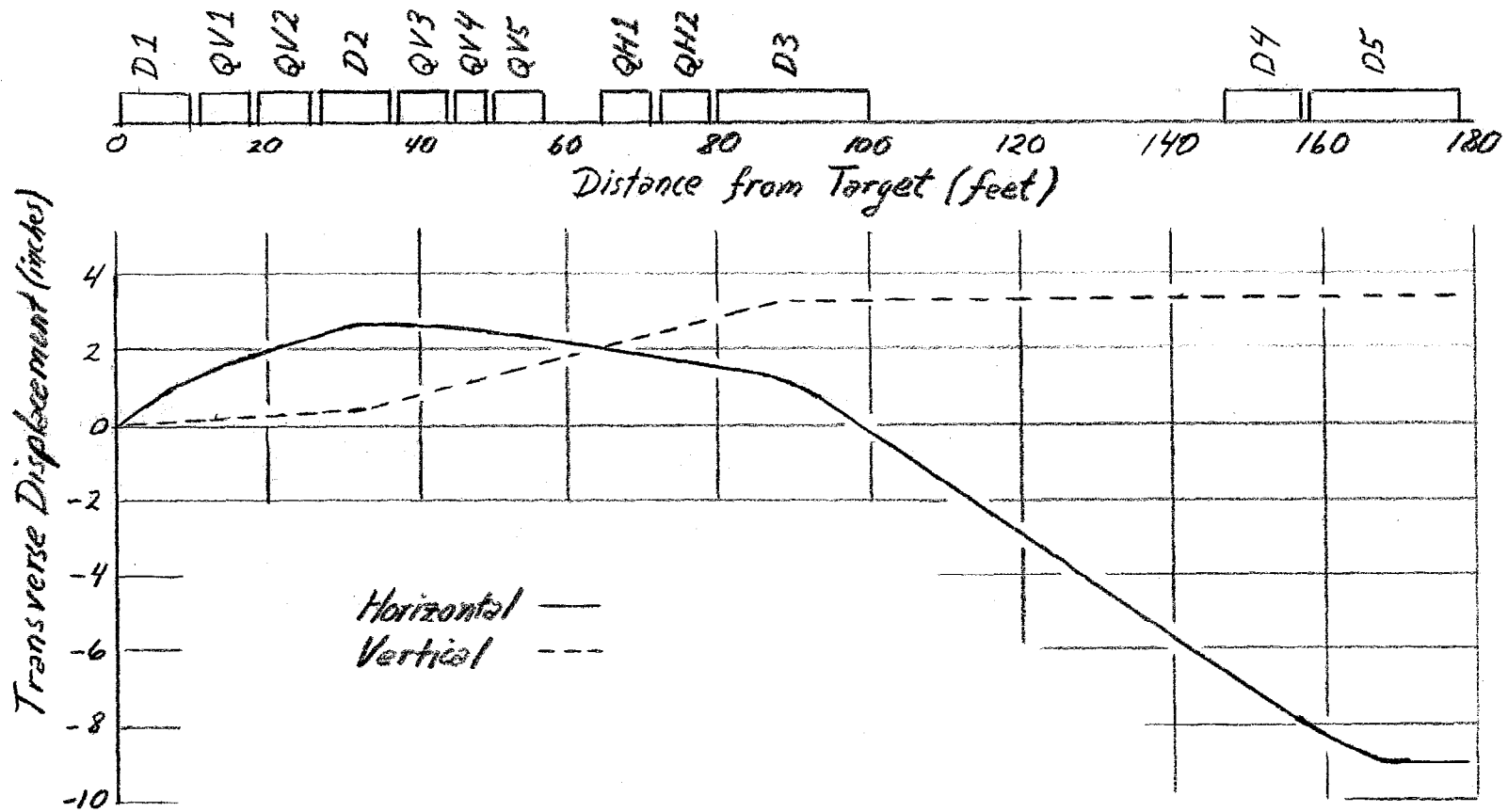


Figure 6. Magnet layout and central trajectory of new beam.

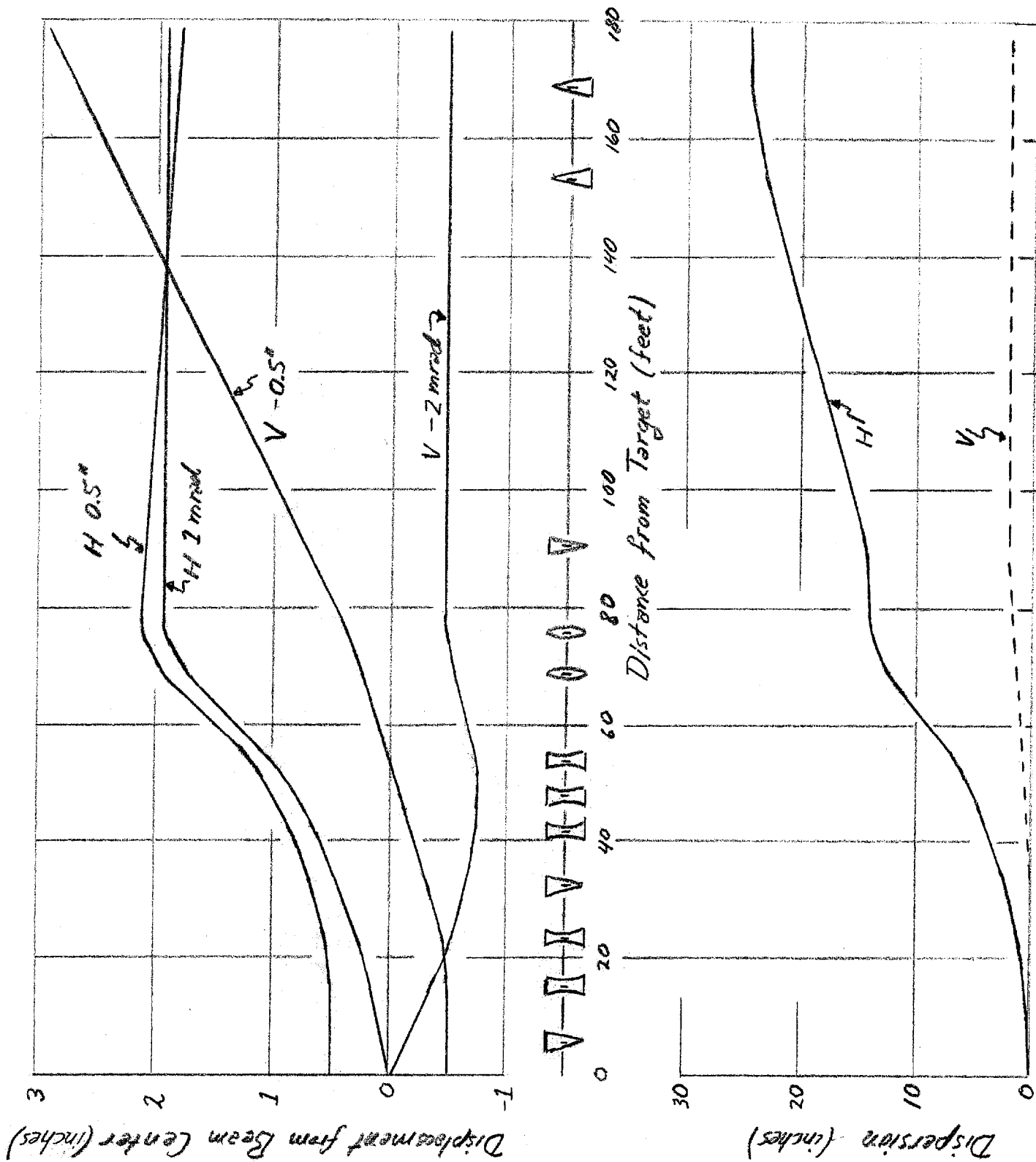


Figure 7. Various rays in proposed beam.

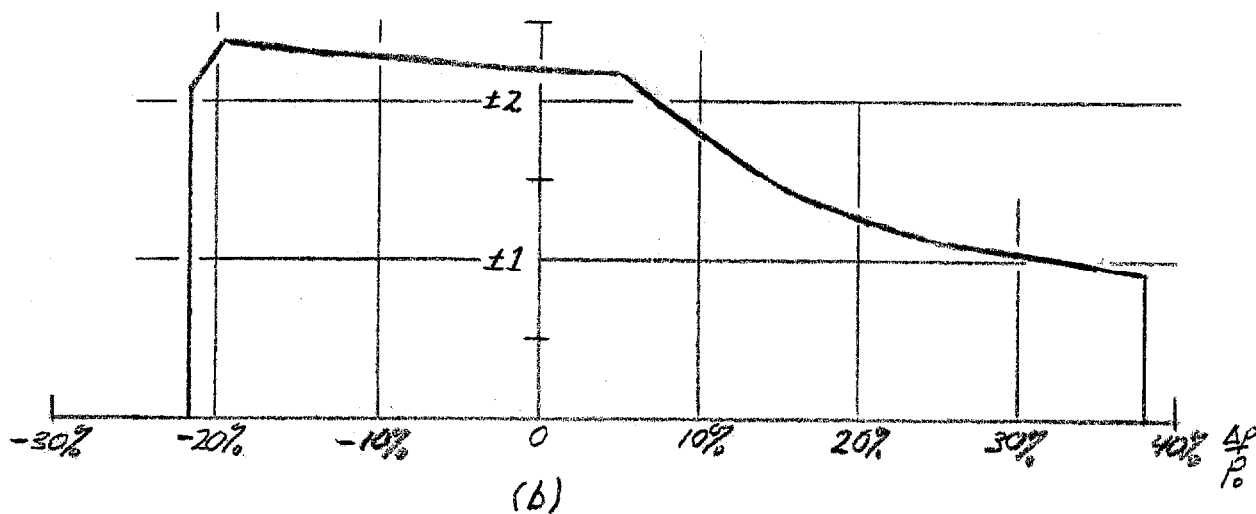
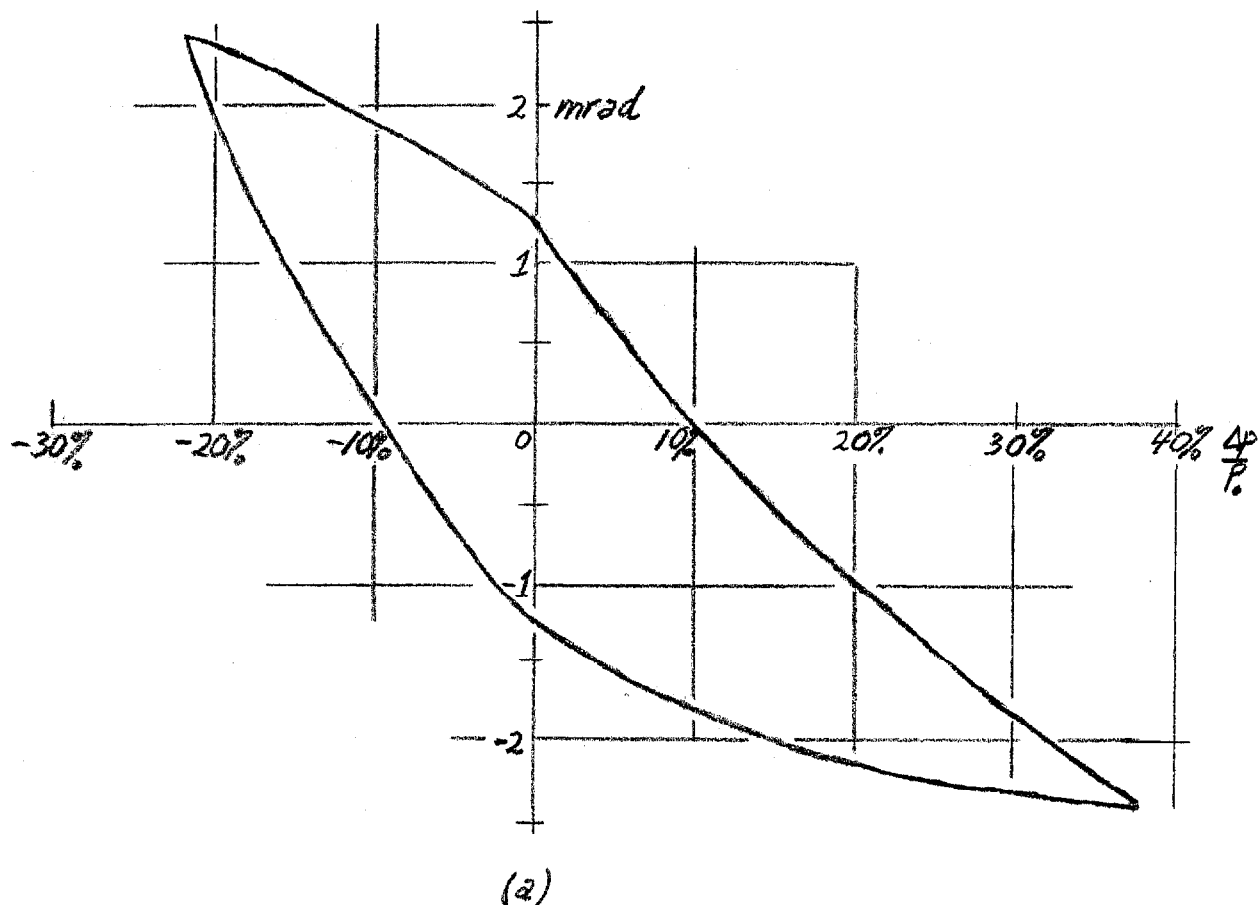


Figure 8. Angular acceptance versus momentum for proposed beam (flat version) in (a) horizontal plane, and (b) vertical plane.

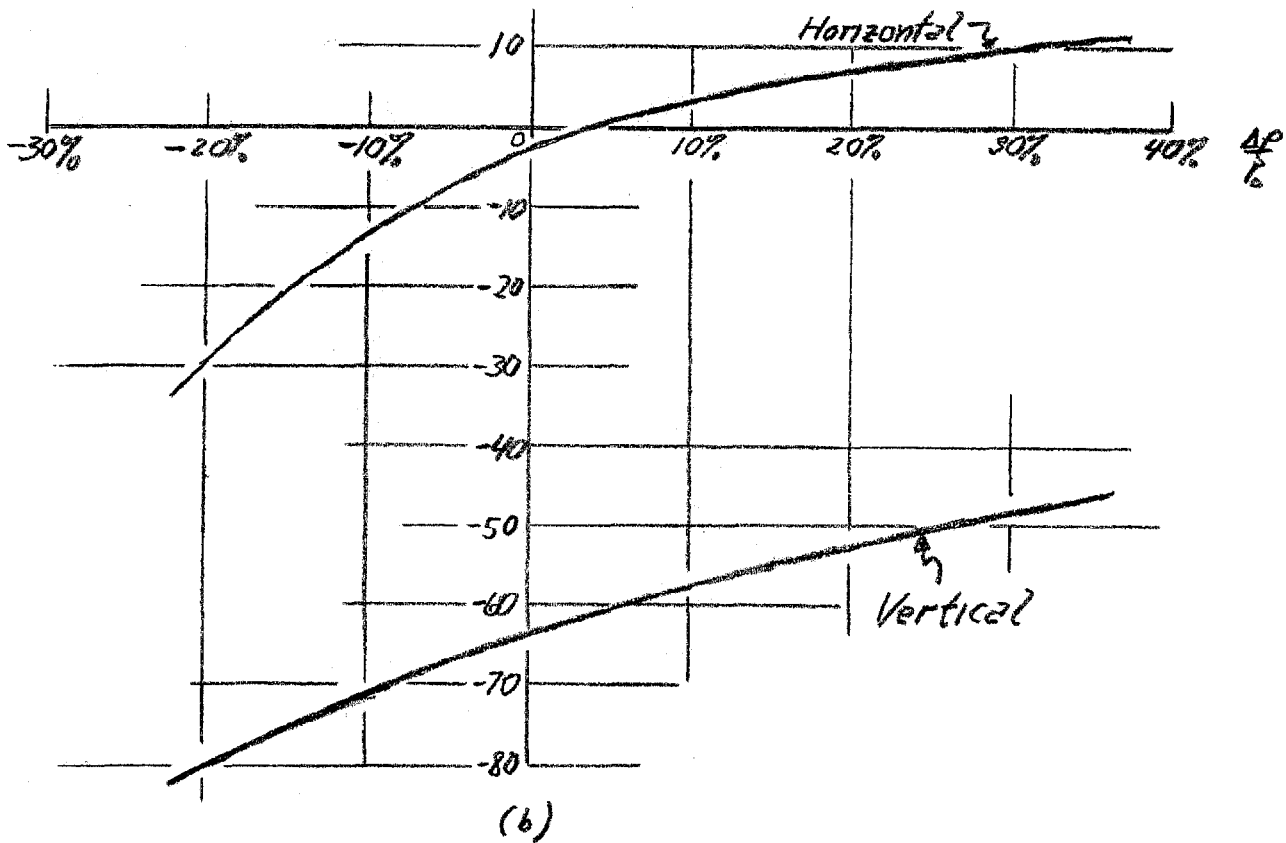
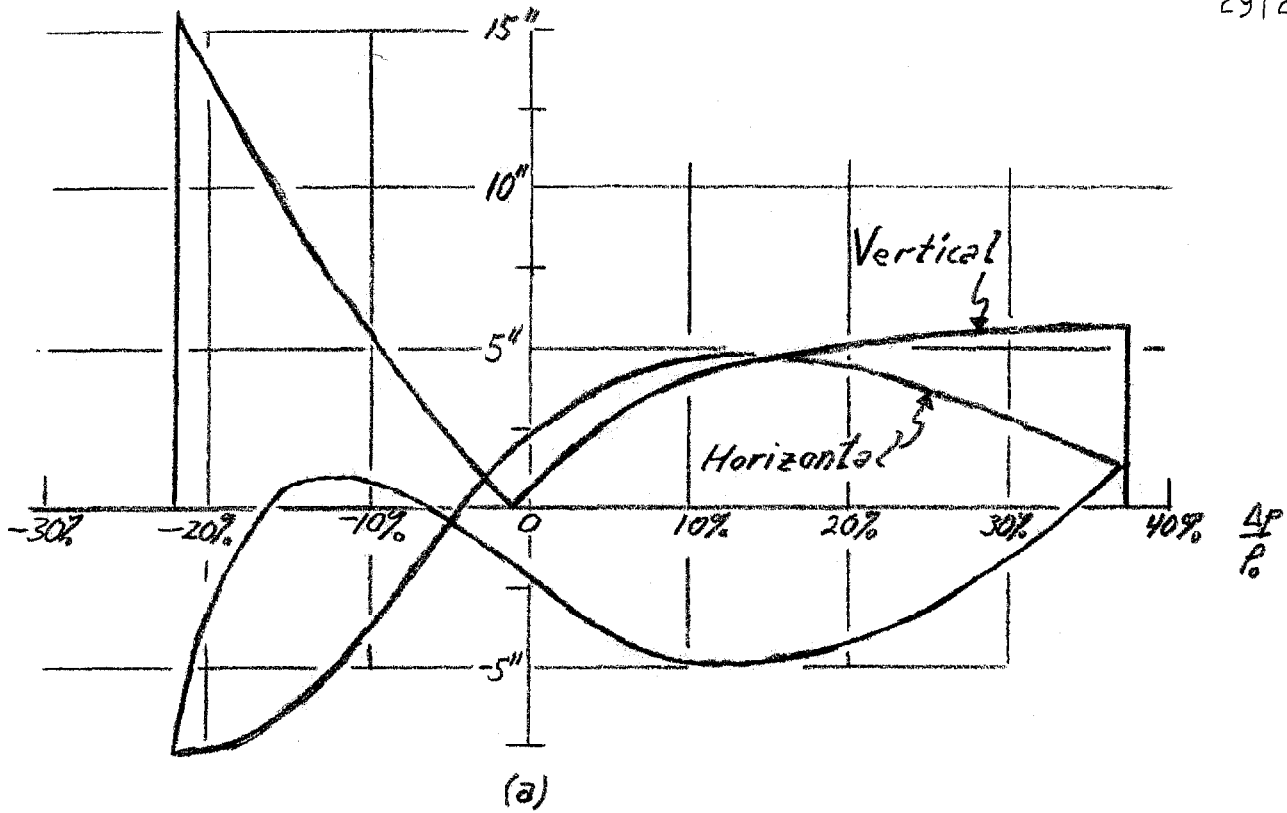


Figure 9. (a) Transverse position boundaries at end of decay tube for new beam. (b) Magnification at end of decay tube.

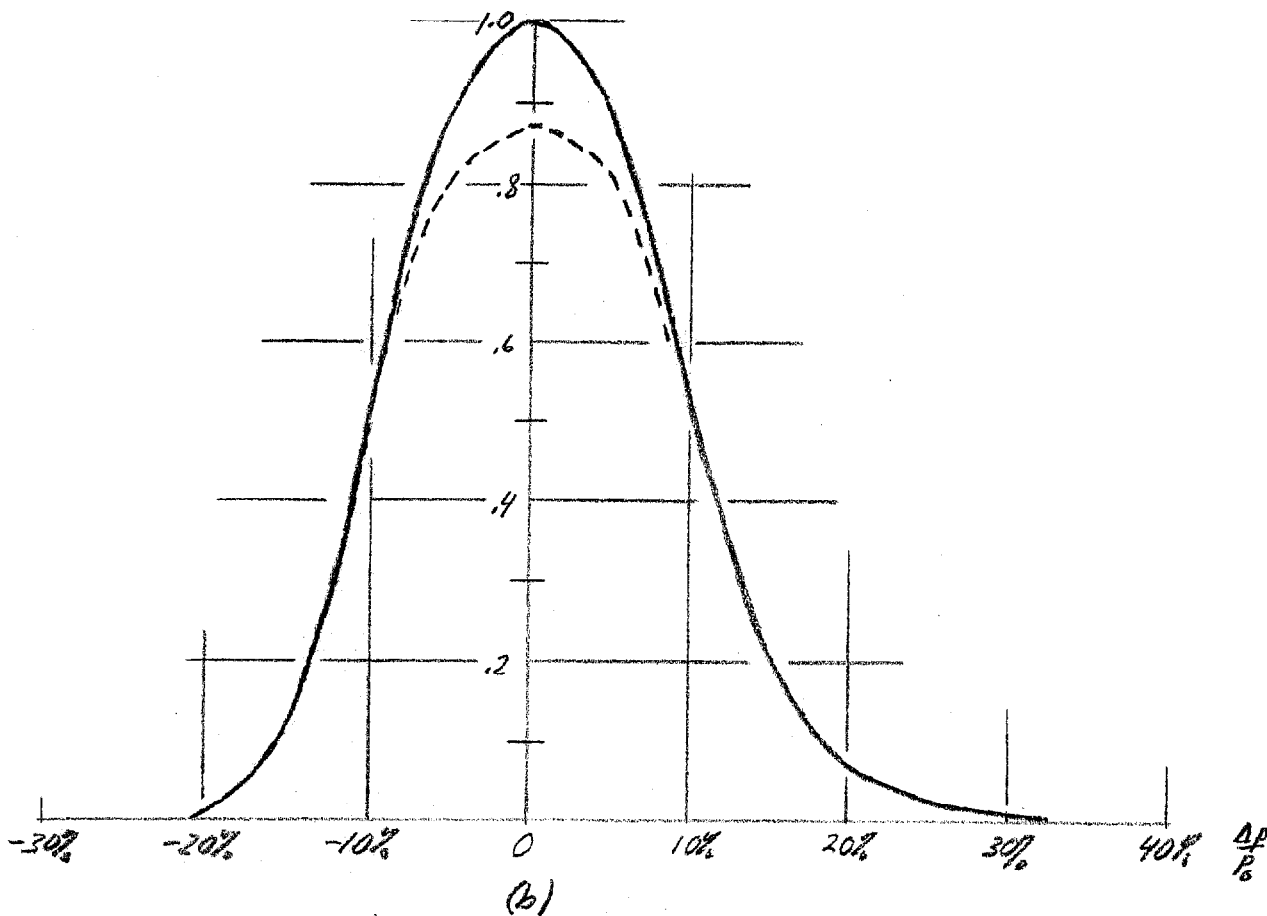
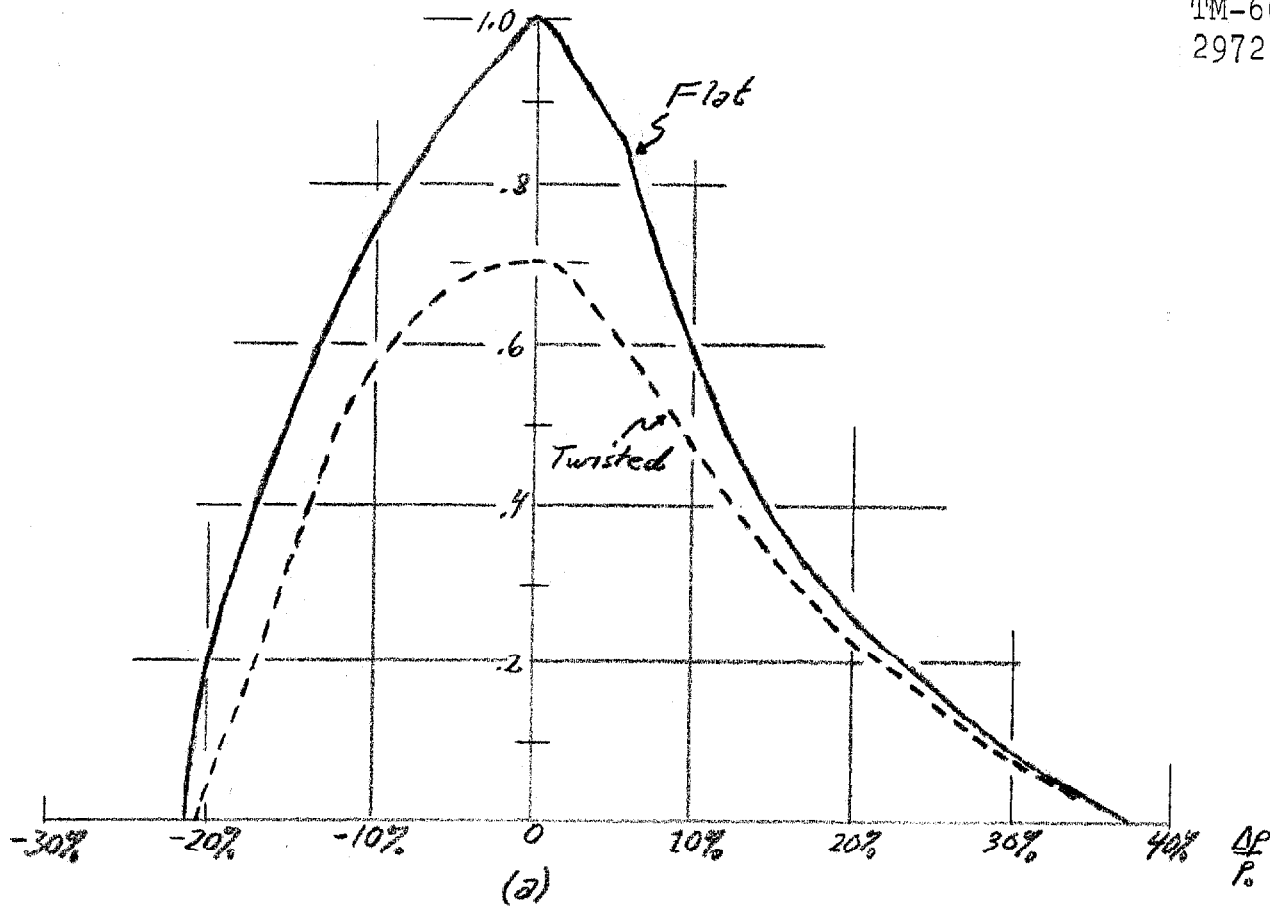
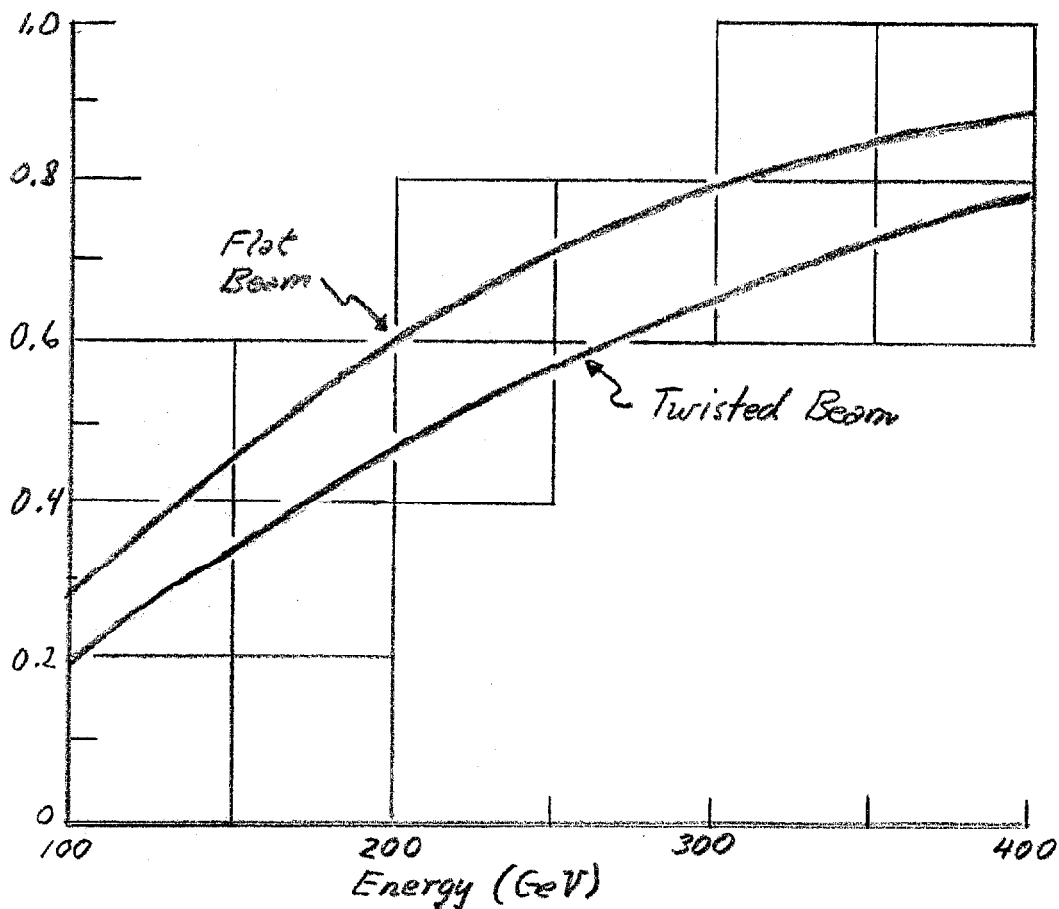
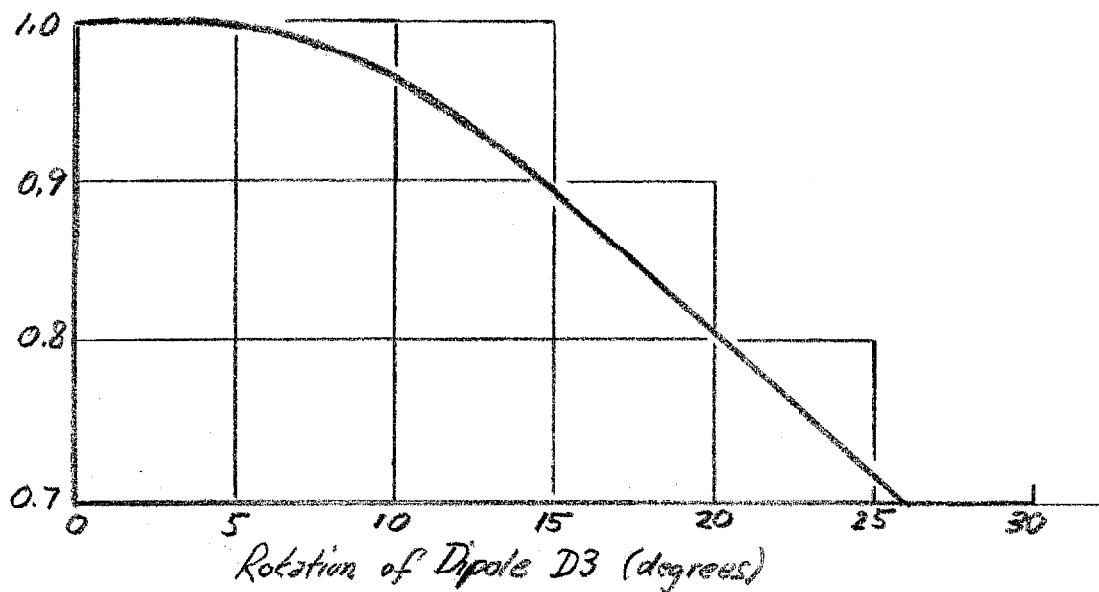


Figure 10. (a) Relative solid angle acceptances of flat and twisted versions of new beam. (b) Relative acceptance of 350 GeV pions.



(a)



(b)

Figure 11. (a) Fraction of pions accepted versus central energy setting. (b) Relative reduction of solid angle at central energy due to rotation of dipole D3.

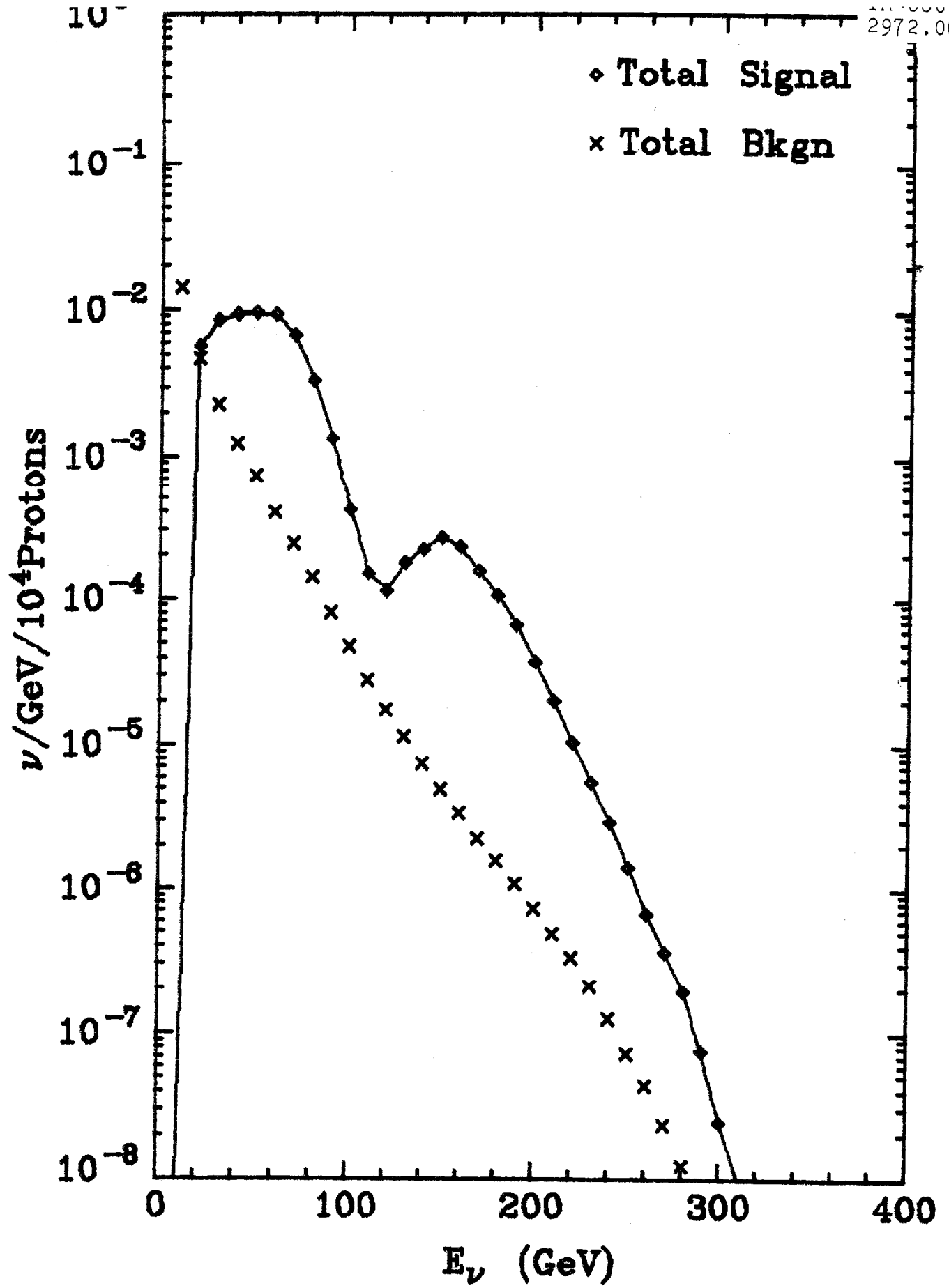


Figure 12. Signal and background neutrino fluxes at Lab-E location with old narrow band beam set to accept negative secondaries at 200 GeV for 400 GeV incident protons.

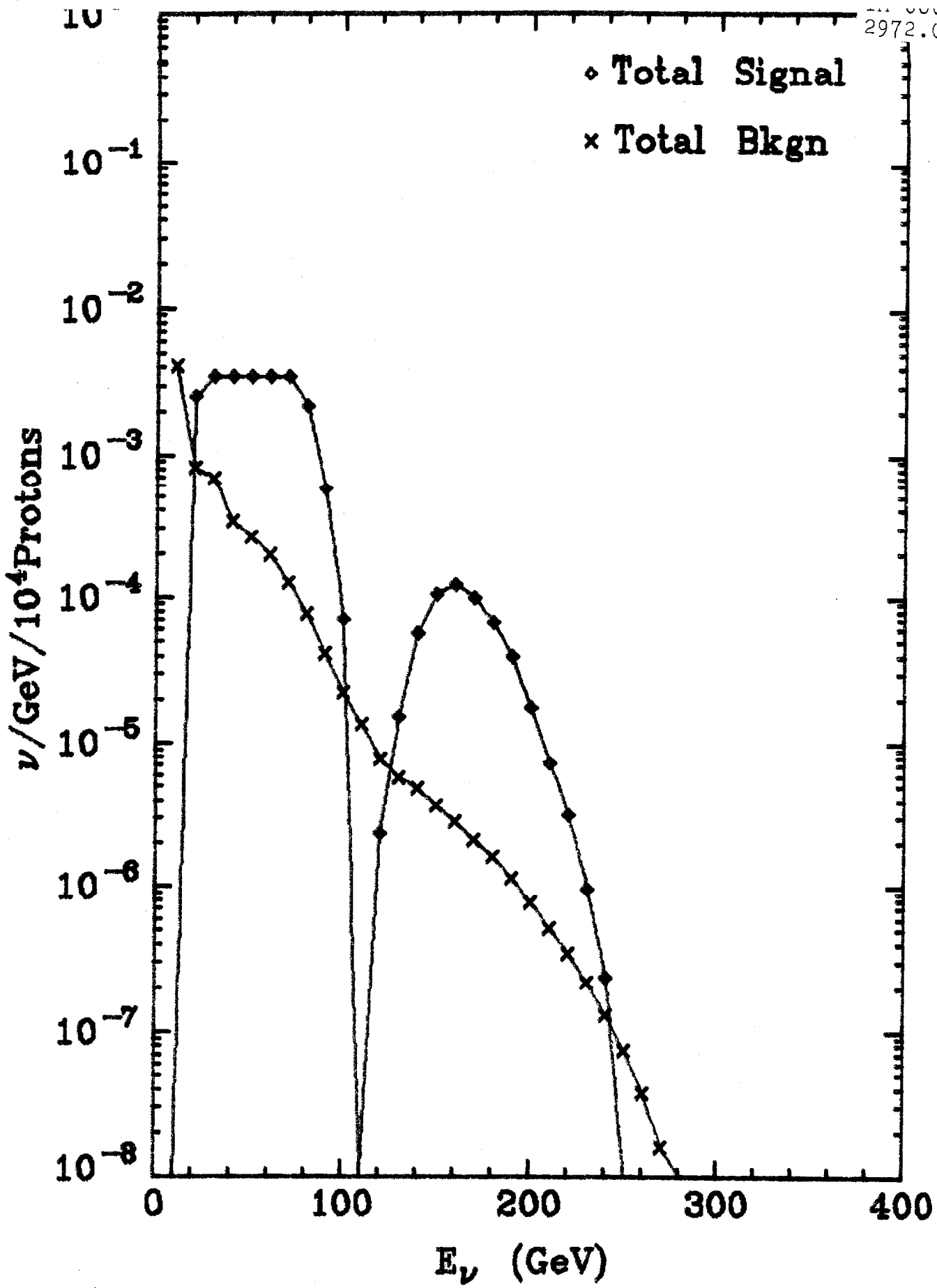


Figure 13. Signal and background neutrino fluxes at Lab-E location with flat version of new beam set to accept negative secondaries at 200 GeV for 400 GeV incident protons.

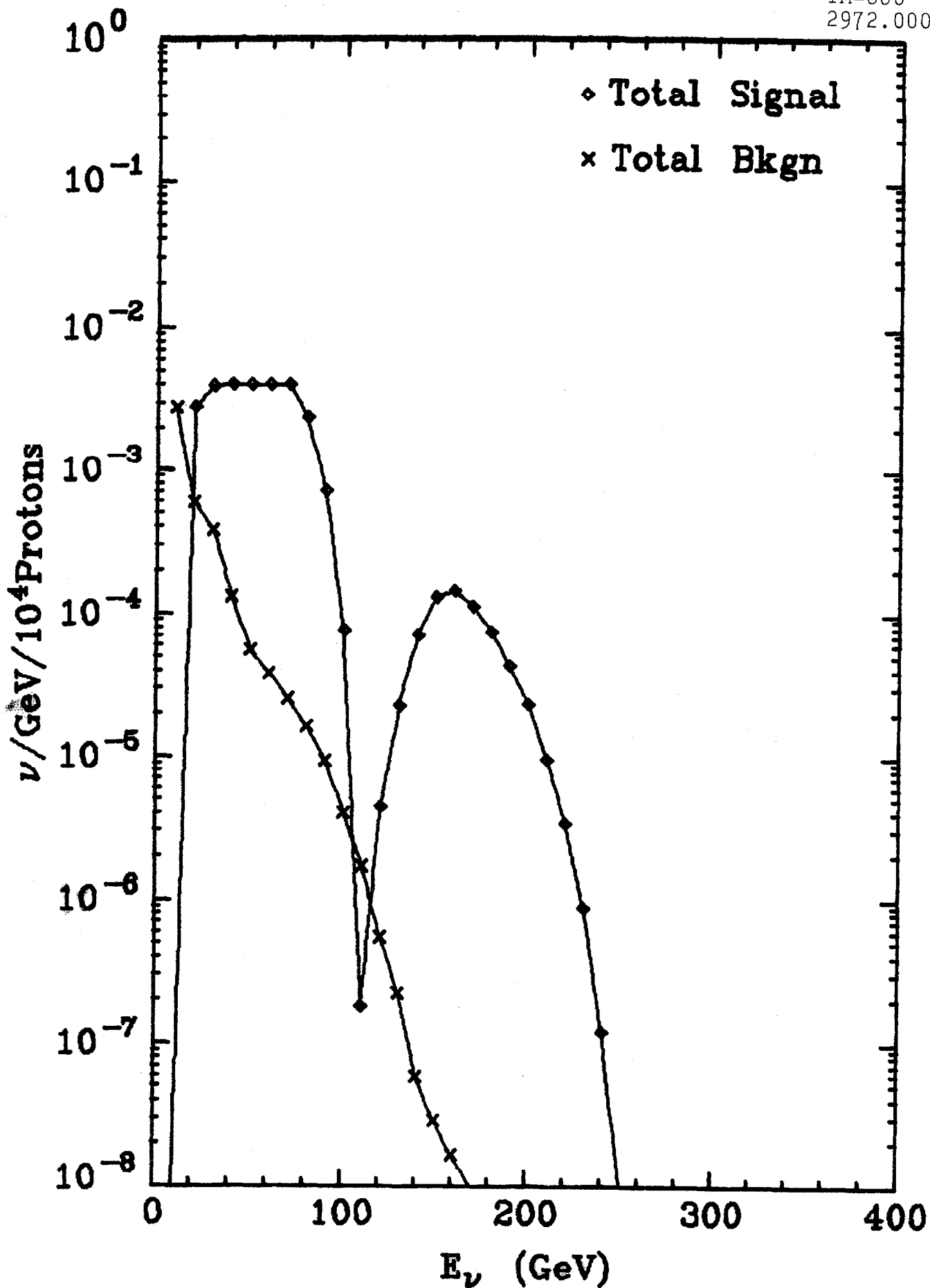


Figure 14. Signal and background neutrino fluxes at Lab-E location with twisted version of new beam set to accept negative secondaries at 200 GeV for 400 GeV incident protons.

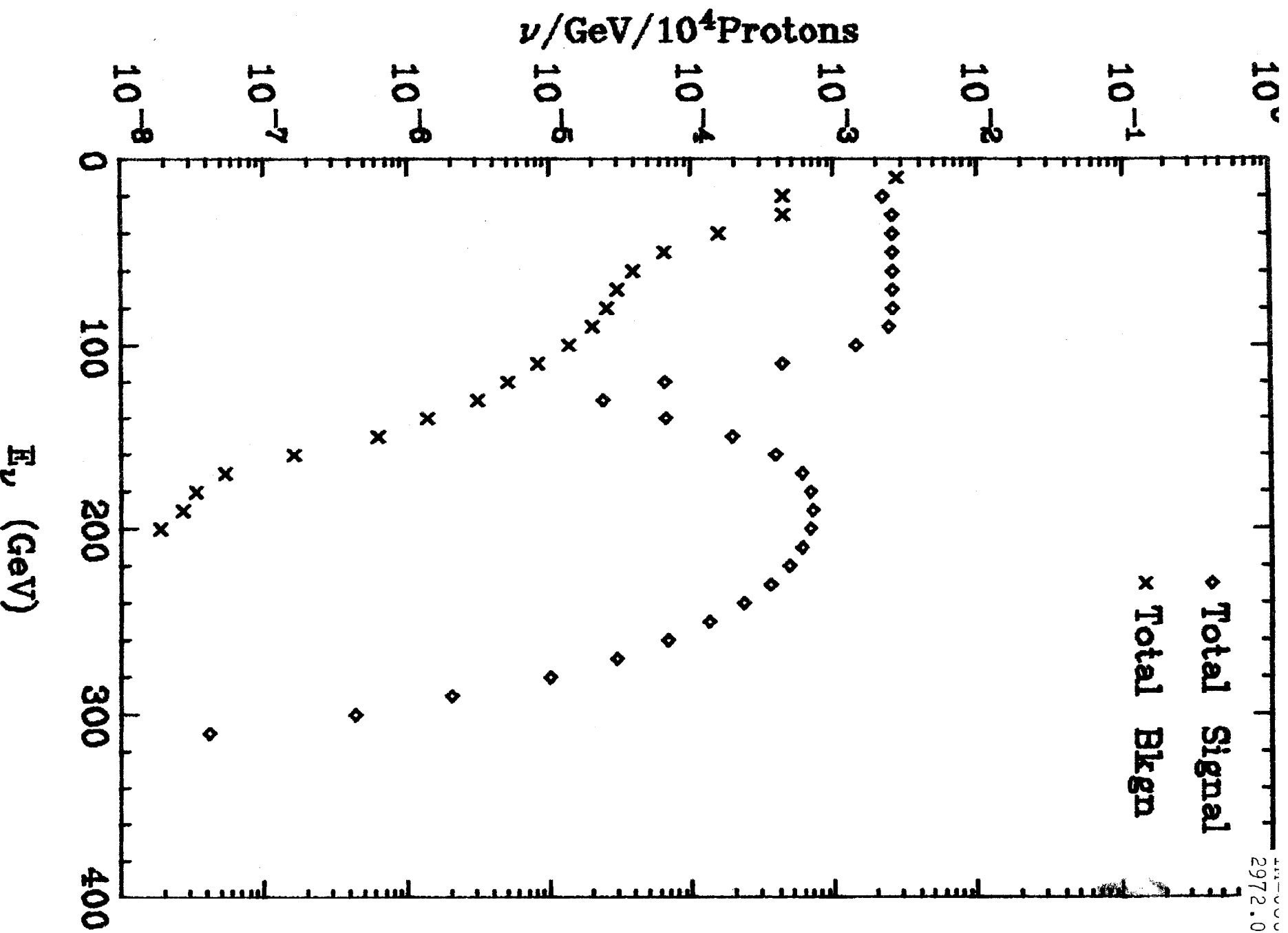


Figure 15. Signal and background neutrino fluxes at Lab-E location with twisted version of new beam set to accept positive secondaries at 250 GeV for 400 GeV incident protons.

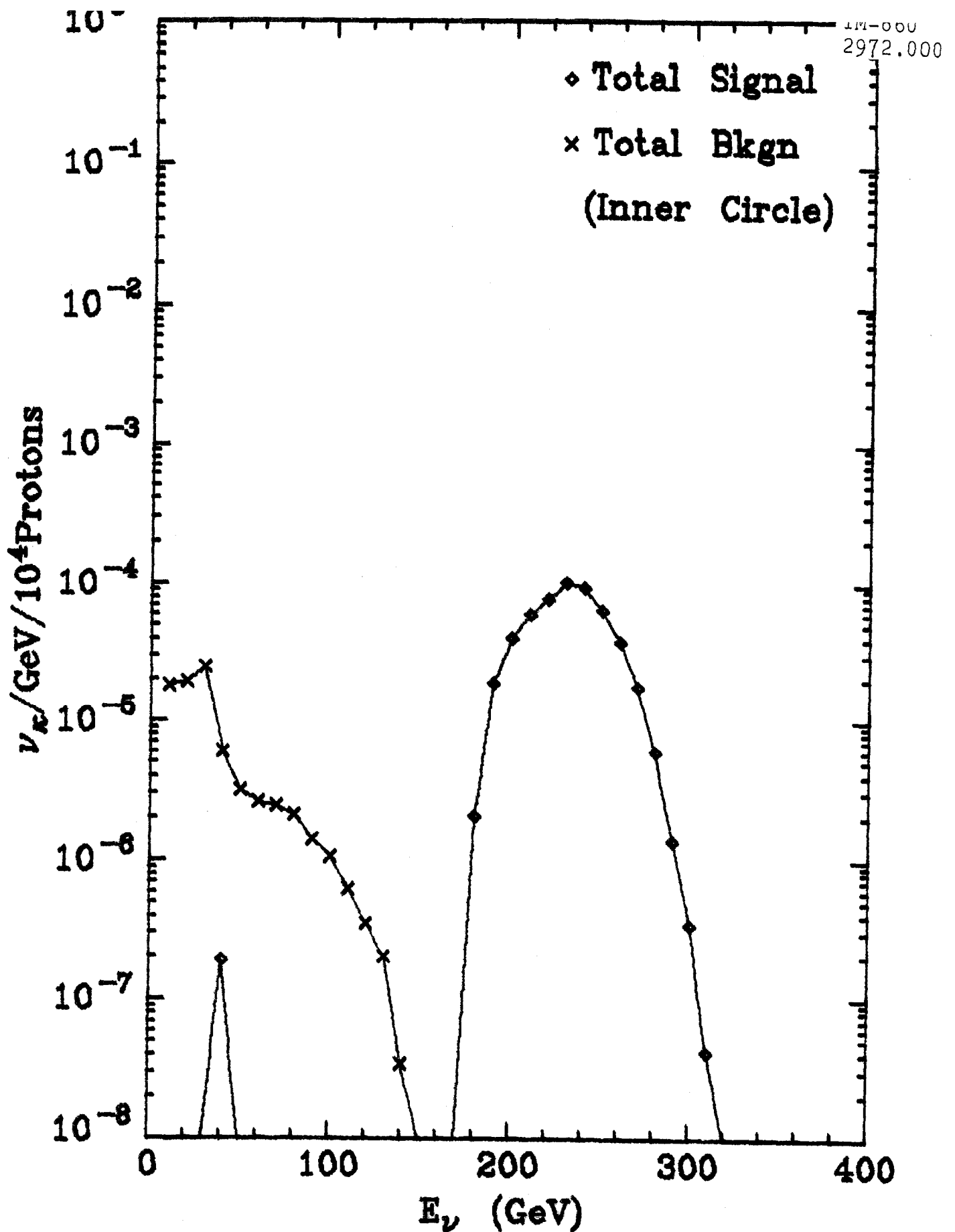


Figure 16. Signal and background neutrino fluxes from kaon decays incident on the target calorimeter at the Lab-E location within a circle of radius 0.42 m about the center line of the apparatus. Twisted version of new beam is set to accept 250 GeV secondaries with 400 GeV primary protons striking the meson production target.